Research Article

Molecular Cancer Therapeutics

BNC105: A Novel Tubulin Polymerization Inhibitor That Selectively Disrupts Tumor Vasculature and Displays Single-Agent Antitumor Efficacy

Gabriel Kremmidiotis, Annabell F. Leske, Tina C. Lavranos, Donna Beaumont, Jelena Gasic, Allison Hall, Michael O'Callaghan, Clayton A. Matthews, and Bernard Flynn

Abstract

Vascular disruption agents (VDA) cause occlusion of tumor vasculature, resulting in hypoxia-driven tumor cell necrosis. Tumor vascular disruption is a therapeutic strategy of great potential; however, VDAs currently under development display a narrow therapeutic margin, with cardiovascular toxicity posing a dose-limiting obstacle. Discovery of new VDAs, which display a wider therapeutic margin, may allow attainment of improved clinical outcomes. To identify such compounds, we used an *in vitro* selectivity screening approach that exploits the fact that tumor endothelial cells are in a constant state of activation and angiogenesis and do not undergo senescence. Our effort yielded the compound BNC105. This compound acts as a tubulin polymerization inhibitor and displays 80-fold higher potency against endothelial cells that are actively proliferating or are engaged in the formation of *in vitro* capillaries compared with nonproliferating endothelial cells or endothelium found in stable capillaries. This selectivity was not observed with CA4, a VDA currently under evaluation in phase III clinical trials. BNC105 is more potent and offers a wider therapeutic window. CA4 produces 90% vascular disruption at its no observed adverse event level (NOAEL), whereas BNC105 causes 95% vascular disruption at 1/8th of its NOAEL. Tissue distribution analysis of BNC105 in tumor-bearing mice showed that while the drug is cleared from all tissues 24 hours after administration, it is still present at high concentrations within the solid tumor mass. Furthermore, BNC105 treatment causes tumor regressions with complete tumor clearance in 20% of treated animals. *Mol Cancer Ther; 9(6); 1562–73. ©2010 AACR.*

Introduction

Molecules that bind to different sites within the tubulin polymer can produce varied molecular outcomes and confer anticancer activity in diverse tumor indications. Tubulin-binding agents can be classified as tubulin stabilizers or tubulin destabilizers. A tubulin-binding site that affects stabilization has been defined by the interaction of taxanes. A large number of natural products and small-molecule compounds have been shown to have their effect via the taxane binding site, promoting tubulin polymerization and stabilization of microtubules (1). Disparate to the taxane site, the binding of *Vinca* alkaloids to the tubulin polymer occurs at a site that mediates tubulin destabilization. Colchicine interactions with tubulin define an additional binding site that also causes tubulin destabilization (2).

Although agents binding to the taxane and *Vinca* sites have been successfully used as anticancer chemotherapeutics, by comparison the colchicine-site binders have been relatively neglected, possibly due to the poor therapeutic margin exhibited by colchicine. Recently, several agents have been described that bind at the colchicine site and are capable of causing blood vessel disruption within solid tumors. This class of compounds is defined as vascular disruption agents (VDA). Many of the colchicine-site binding agents that exhibit VDA capability were based on natural products such as combretastatins (CA4P, OXi-4503, and AVE-8062), colchicines (ZD6126), and phenylahistin (NPI-2358), whereas others were discovered independently (MN-029 and EPC2407; refs. 3, 4).

The preclinical evaluation of tubulin-targeting VDAs has shown that these compounds are able to disrupt tumor blood flow, causing tumor hypoxia and necrosis (5). However, this vascular disruption spares the outer cellular rim of the tumor mass, which seems to be supported by normal blood vessels that surround the tumor capsule and remain unaffected by VDA action (6). It is believed that this viable rim mediates recovery from the vascular damage caused by VDA treatment (6).

Authors' Affiliation: Bionomics Ltd., Thebarton, South Australia, Australia

Note: Supplementary material for this article is available at Molecular Cancer Therapeutics Online (http://mct.aacrjournals.org/).

Corresponding Author: Gabriel Kremmidiotis, Bionomics Limited, 31 Dalgleish Street, Thebarton, 5031 South Australia, Australia. Phone: 61-8-8354-6123; Fax: 61-8-8354-6199. E-mail: gkremmid@bionomics.com.au

doi: 10.1158/1535-7163.MCT-09-0815

Preclinical evidence suggests that VDAs are not effective at stopping tumor growth when used as single agents but may synergize with conventional chemotherapeutics or antiangiogenic agents (7).

Experience with colchicine-site binders such as CA4P and ZD6126 in a clinical setting has shown their ability to disrupt blood flow within human tumors (8, 9). However, negative side effects, such as cardiotoxicity, have resulted in the discontinuation of the clinical development of ZD6126 (9). Nevertheless, CA4P remains in development and is currently undergoing evaluation in phase III clinical trials for anaplastic thyroid carcinoma (FACT trial #NCT00507429) and for nonsquamous non–small cell lung cancer (FALCON trial #NCT00653939).

Further improvement in the therapeutic window displayed by current VDAs may be achieved by exploiting the fact that tumor endothelial cells are in a constant state of activation and angiogenesis and do not undergo senescence (10). We constructed a chemical library of more than 100 compounds based on diversification of the combretastatin pharmacophore. We used two *in vitro* correlates of endothelial cell function to screen this library for compounds that exhibit selectivity for endothelial cells that are in a state of activation or angiogenesis. This effort led to the discovery of a novel tubulin-targeting agent, BNC105. The data presented in this report show that BNC105 exhibits a wider therapeutic window than CA4P. This increased therapeutic window enables administration of BNC105 at higher dose levels, yielding single-agent efficacy in human xenograft tumor models.

Materials and Methods

Cell culture and cell lines

All *in vitro* assays were carried out using endothelial cells derived from human umbilical vein (HUVEC; Clonetics, Lonza) or human abdominal aorta (HAAE-1; American Type Culture Collection). HUVEC were routinely cultured in EGM-2 medium (Clonetics) and HAAE-1 cells were cultured in F12K medium (Gibco, Invitrogen) containing 10% FCS, 0.1 mg/mL heparin (Sigma-Aldrich), 0.03 mg/mL endothelial cell growth supplement (Sigma-Aldrich), 2 mmol/L penicillin-streptomycin-glutamine (Gibco, Invitrogen), and 10 mmol/L HEPES buffered solution (Gibco, Invitrogen). Cell cultures between passages 2 and 6 were used for all assays. Cancer cell lines included Calu 6, DU145, Colo 205 (American Type Culture Collection), and MDA-MB-231 (kind gift from the Women's and Children's Hospital, Adelaide, Australia). Calu 6 and DU145 cells were cultured in MEM (Gibco) with 10% FCS, 2 mmol/L penicillin-streptomycin-glutamine, 10 mmol/L HEPES buffered solution, 1 mmol/L sodium pyruvate solution (Gibco), and 0.1 mmol/L nonessential amino acids solution (Gibco). Colo 205 cells were cultured in RPMI 1640 (Gibco) with 10% FCS and 2 mmol/L penicillin-streptomycin-glutamine. MDA-MB-231 cells were cultured in RPMI 1640 (Gibco) with 10% FCS, 2 mmol/L penicillin-streptomycin-glutamine, and 10 mmol/L HEPES buffered solution. All cells were cultured in a humidified incubator at 37°C with 5% CO_2.

Endothelial cell proliferation assay

HUVEC or HAAE-1 cell cultures were exposed to a concentration range of 0.1 to 1,000 nmol/L for each test compound tested. Proliferation assays were carried out in triplicate in 96-well plates. For activated growth conditions, HUVEC and HAAE-1 cells were seeded at 2,500 and 5,000 per well, respectively, and cultured in EGM-2 or medium containing 0.03 mg/mL endothelial cell growth supplement (Sigma-Aldrich) as described above. For quiescent growth conditions, HUVEC and HAAE-1 cells were seeded at 15,000 and 5,000 per well, respectively, in basal medium (EBM-2 or F12K) containing 0.5% FCS and antibiotics. Cells were allowed to adhere overnight followed by incubation with compounds under evaluation for 48 hours. Metabolically active cells were measured using CellTiter 96 Aqueous One Solution (Promega Corp.) according to the manufacturer's instructions, and absorbance readings taken at 492 nm. Control absorbance readings for quiescent endothelial cells remained relatively unchanged over the 48-hour culture period. Absorbance readings for each compound concentration were normalized to corresponding vehicle control cultures. A sigmoidal dose-response curve was fitted to the data, and the concentration at which proliferation decreased by 50% was calculated using GraphPad Prism 4 software (San Diego).

Capillary formation and disruption assays

Capillary formation assays were conducted in 96-well plates using HUVEC and HAAE-1 cells plated on a Matrigel layer (BD Biosciences) with 25,000 and 20,000 cells per well, respectively, and incubated for 22 hours. Capillary disruption assays were carried out in a 96-well plate format using HUVEC cells plated at 25,000 per well in EGM-2 medium on a Matrigel layer (BD Biosciences). Capillaries were allowed to form over a 16-hour period before the addition of test compound or control. Cells were stained using calcein AM (Calbiochem) at room temperature for 40 minutes after a brief washing step. Images were acquired immediately following compound addition and 5 hours after exposure to test compound. Tube formation was quantified by measuring the length of capillary structures using the software NIH ImageJ.

Tubulin polymerization assays

In vitro tubulin polymerization assays were done using a Tubulin Polymerization Assay Kit (Cytoskeleton, Inc.) in a 384-well format, which used the polymerization of bovine neuronal tubulin *in vitro* in the presence of varying concentrations of BNC105 or CA4. Fluorescence measurements were obtained at 1-minute intervals over a 42-minute period. Fluorescent measurements were

taken following excitation at 360 nm, and emission was measured at 420 nm using a BMG Flurostar fluorescent plate reader. Data were analyzed as relative fluorescent units.

F-Actin staining and immunohistochemical analysis

HUVEC were plated on glass coverslips in a six-well plate at 7.5×10^4 cells per well in EGM-2 medium and incubated overnight. On the following day, cells were 50% to 60% confluent and the cell medium was replaced with EGM-2 medium containing 10 nmol/L BNC105 or 0.1% DMSO vehicle control. Cells were incubated for 20 minutes at 37°C before being fixed in 3.7% formaldehyde/PBS solution for 10 minutes at room temperature and then permeabilized in 0.5% Triton X-100/PBS solution for 5 minutes at 4°C. Following permeabilization, FITC-phalloidin (Sigma-Aldrich) was added to each well at 1 μg/mL in PBS and incubated in darkness for 1 hour. Coverslips were mounted on glass slides using Vectashield containing 4′,6-diamidino-2-phenylindole (Vector Laboratories) and stored in darkness at 4°C. Images of the cells showing F-actin and 4′,6-diamidino-2-phenylindole staining were digitally acquired using the 100× objective lens of an Olympus BX51 microscope and photographed using a charge-coupled device camera (Optronics).

Endothelial monolayer permeability assay

The permeability of an endothelial cell monolayer was assessed using an *In Vitro* Vascular Permeability Assay Kit (Chemicon, Millipore) as previously described (11). Briefly, HUVEC were plated at 5×10^4 cells per insert in EGM-2 medium and incubated for 48 hours to reach 100% confluency. BNC105 or CA4 were diluted in EGM-2 medium and added to the upper chamber of the apparatus. Following 15 minutes of incubation, the compounds were removed and FITC-conjugated dextran was added for 5 minutes. Fluorescent measurements of the lower chamber were taken after excitation at 520 nm, and emission was measured at 485 nm using a BMG Fluorstar fluorescent plate reader. Data were analyzed as relative fluorescent units.

Pharmacokinetics and metabolism assays

For *in vivo* studies, all the animals were housed under pathogen-free conditions and cared for in accordance with the NHMRC guidelines and the Australian Code of Practice for the Care and Use of Animals for Scientific Purposes. To facilitate i.v. administration of BNC105, the phosphate ester of this compound was synthesized (BNC105P) and dissolved in isotonic saline (Table 1B). Pharmacokinetic studies were conducted by bolus tail-vein i.v. administration of BNC105P to nonfasting male Swiss mice. Postadministration blood samples were collected into tubes containing anticoagulant and a protease inhibitor cocktail via cardiac puncture up to 6 hours post-dose. Blood plasma was separated by centrifugation and frozen until analysis. Extracts were prepared and analyzed by high-performance liquid chromatography-mass spectrometry (HPLC-MS) against a standard curve. Pharmacokinetic variables were determined using a noncompartmental method (WinNonLin). Metabolism assays were conducted using recombinant CYP450 Supersomes. BNC105 and

Table 1. BNC105 is a CA4 analogue that selectively inhibits the proliferation of activated endothelial cells

A

Compound	Activated EC_{50}	Quiescent EC_{50}	Selectivity ratio, quiescent/activated
HUVEC			
BNC105	0.31 nmol/L	25 nmol/L	80.6
0075	0.36 nmol/L	2.7 nmol/L	7.5
0079	3.28 nmol/L	186 nmol/L	56.7
CA4	3.6 nmol/L	3.9 nmol/L	1.1
Paclitaxel	2.63	2.73	1
Vinblastine	0.86	1.03	1.2
Vincristine	2.16	1.76	0.8
HAAEC			
BNC105	0.1 nmol/L	12 nmol/L	120
CA4	2.2 nmol/L	1.3 nmol/L	0.6

B

Compound	Structure	Compound	Structure
BNC105	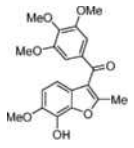	CA4	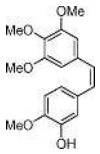
BNC105P	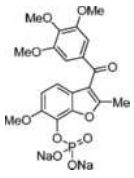	CA4P	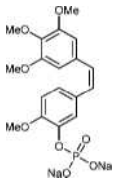

NOTE: A, measurement of the activity of BNC105, two chemically related compounds (0075 and 0079), CA4, paclitaxel, vinblastine, and vincristine on the proliferation of activated and quiescent HUVEC and HAAEC. EC_{50} values are based on three replicates obtained following a 48-h exposure to increasing doses of compound. Cell proliferation was determined using CellTitre 96 Aqueous One Reagent (Promega) and calculated relative to vehicle control. B, structure of BNC105, the prodrug BNC105P, and the comparator CA4 with its prodrug CA4P.

BNC105P were added to Supersomes incubation solutions to a final concentration of 1 μmol/L and incubated at 37°C with required cofactors for 10 minutes before the addition of the NADPH-regenerating system. Samples were taken throughout the 45-minute incubation period and quenched with 100% acetonitrile containing diazepam as an analytic internal standard. Analysis of samples was done by mass spectrometry on Micromass Q-TOF Micro and Micromass Quattro Ultima Pt triple quadrupole instruments for BNC105 and BNC105P, respectively, coupled to a Waters 2795 HPLC device. The *in vitro* clearance values were calculated and expressed relative to the CYP450 content during incubation.

Vascular disruption assay

Female BALB/c nu/nu mice at 6 to 8 weeks [Animal Resources Centre (ARC), Perth, Australia] were injected s.c. with human cancer cell lines representing breast (MDA-MB-231), lung (Calu 6), colon (Colo 205), or prostate (DU145) cancer. Cells were resuspended in Dulbecco's PBS (Sigma-Aldrich) and 2×10^6 cells in 50 μL of PBS were s.c. injected in the hind flank (Calu 6, Colo 205, and DU145) or near the mammary fat pad (MDA-MB-231). Tumors were grown to an average size of 300 mm^3 before treatment. BNC105P treatment consisted of a single i.v. injection at dose levels ranging from 1 to 150 mg/kg. Saline treatment was included as a vehicle control. Twenty-four hours after the injection of the compound, animals were i.v. injected with 10 mg/kg of H33342 Hoechst fluorescent dye (Invitrogen), which acts as a marker of blood perfusion in tumors and normal tissues (12). After 1 minute, animals were euthanized and tumors were excised for histologic examination in optimum cutting temperature compound (Tissue-Tek, Sakura Finetek). Images of histologic sections were captured and assembled using MW Snap software version 3.0.0.74 (Mirek Wojtowicz) and Motic Images Assembly 1.0 Pro (Motic China Group Co. Ltd.). Quantification of H33342 Hoechst and terminal deoxyribonucleotidyl transferase–mediated dUTP nick end labeling (TUNEL) staining was done using the software NIH ImageJ.

BNC105 tissue distribution assay

Female BALB/c nu/nu mice at 6 weeks (ARC) were s.c. inoculated with human MDA-MB-231 breast cancer cells. Tumors were grown to an average size of 200 mm^3 before a single bolus i.v. injection of 10 mg/kg BNC105P was administered. Tumors and tissues (liver, kidney, heart, brain, and spleen) were harvested and snap-frozen at 15 minutes and 2, 6, and 24 hours after administration ($n = 3$ per time point). Tissues were homogenized and prepared using protein precipitation with acetonitrile. Supernatants containing BNC105 were subsequently analyzed by HPLC-MS on a Quattro Premier triple quadrupole mass spectrometer. Sample concentrations were determined against calibration standards prepared in acetonitrile-water.

Tumor growth inhibition assay

Female BALB/c nu/nu mice at 6 to 8 weeks (ARC) were s.c. inoculated with human cancer cell lines derived from lung (Calu 6) and breast (MDA-MB-231) cancers. Tumors were grown to an average size of 200 mm^3 before commencing treatment. BNC105P at dose levels ranging from 10 to 80 mg/kg and saline vehicle control were administered by i.v. injection as described. Tumor volume (in cubic millimeters) was measured two to three times per week. Animals were euthanized if tumor volume exceeded 2,000 mm^3.

Statistical analyses

Results from tumor growth inhibition assays were analyzed for statistical significance using two-tailed *t* tests ($P < 0.05$) and GraphPad Prism version 4 software. Results from VDA analysis were analyzed for statistical significance using one-way ANOVA with post hoc test (Dunnett's).

Results

Identification of BNC105, a compound that exhibits high activity against proliferating endothelial cells and comparatively low activity against quiescent endothelial cells

A library of CA4 chemical analogues was evaluated for cytotoxic activity against growth factor–supplemented endothelial cells and growth factor–deprived endothelial cell cultures. Our analyses identified three compounds that exhibit selectivity for activated endothelial cells. The compound BNC105 exhibited the highest degree of selectivity, being 80 times more active against activated endothelial cells than against quiescent endothelial cells (Table 1A). This degree of selectivity was not observed with CA4, paclitaxel, vinblastine, or vincristine. Furthermore, BNC105 exhibited significantly higher potency than CA4, paclitaxel, vinblastine, or vincristine against actively proliferating endothelial cells (Table 1A). In addition to BNC105, two other compounds in our library with similar structures displayed selectivity for actively proliferating endothelial cells, but to a lesser extent than BNC105 (Table 1A).

To confirm that the selectivity displayed for activated endothelial cells is not restricted to HUVEC, we investigated the activity of BNC105 against activated and quiescent HAAEC HAAE-1 cells. As observed in HUVEC, BNC105 exhibited selectivity for activated HAAEC HAAE-1 cells (Table 1A). This selectivity for activated cells over quiescent cells was not observed with CA4.

BNC105 disrupts the formation of endothelial capillaries but does not disrupt preformed capillaries

We investigated the activity of BNC105 on endothelial cells engaged in capillary tube formation *in vitro*. Endothelial cells were placed on a Matrigel matrix and allowed to form capillary tubes in the presence or absence of compound. Each compound was applied at

concentrations that were shown to display activity in the proliferation assay. Based on our results, BNC105 inhibited the formation of capillary tubes at 1 nmol/L (Fig. 1A). This compound was more potent than CA4, which inhibited capillary formation at 10 nmol/L (Fig. 1B). These results show that BNC105 is highly potent against activated endothelial cells that are engaged in the formation of new capillaries.

Subsequently, we investigated the activity of BNC105 on preformed capillaries. Endothelial cells were plated on Matrigel and allowed to form capillary tubes for 22 hours, followed by exposure to each of the compounds under investigation. Quantification of total capillary length at the 0-hour and the 5-hour time points showed that at the 5-hour time point, there was a 22% decrease in the DMSO control cultures, an 11% decrease in the BNC105 cultures, and a 65% decrease in the CA4 cultures. These results indicate that although BNC105 is capable of inhibiting the formation of capillaries at 1 nmol/L (Fig. 1A), it does not disrupt preformed capillaries at that concentration (Fig. 1C). This result is in agreement with our proliferation assay results, providing further evidence that BNC105 exhibits selectivity for activated endothelial cells. In contrast, CA4 disrupted preformed capillary tubes at 10 nmol/L (Fig. 1D), which is the same concentration required to block the formation of new capillary tubes (Fig. 1B). Staining with calcein AM showed the viability of the cells involved in the *in vitro* capillaries in this assay.

BNC105 is a tubulin polymerization inhibitor

To confirm that BNC105 acts as a tubulin polymerization inhibitor, we tested its ability to alter the dynamics of tubulin polymerization *in vitro*. The change in fluorescence that occurs when tubulin monomers form elongated fibers was used as a measure of tubulin polymerization. Using CA4 as a positive control, BNC105 was shown to inhibit tubulin polymerization (Fig. 2A).

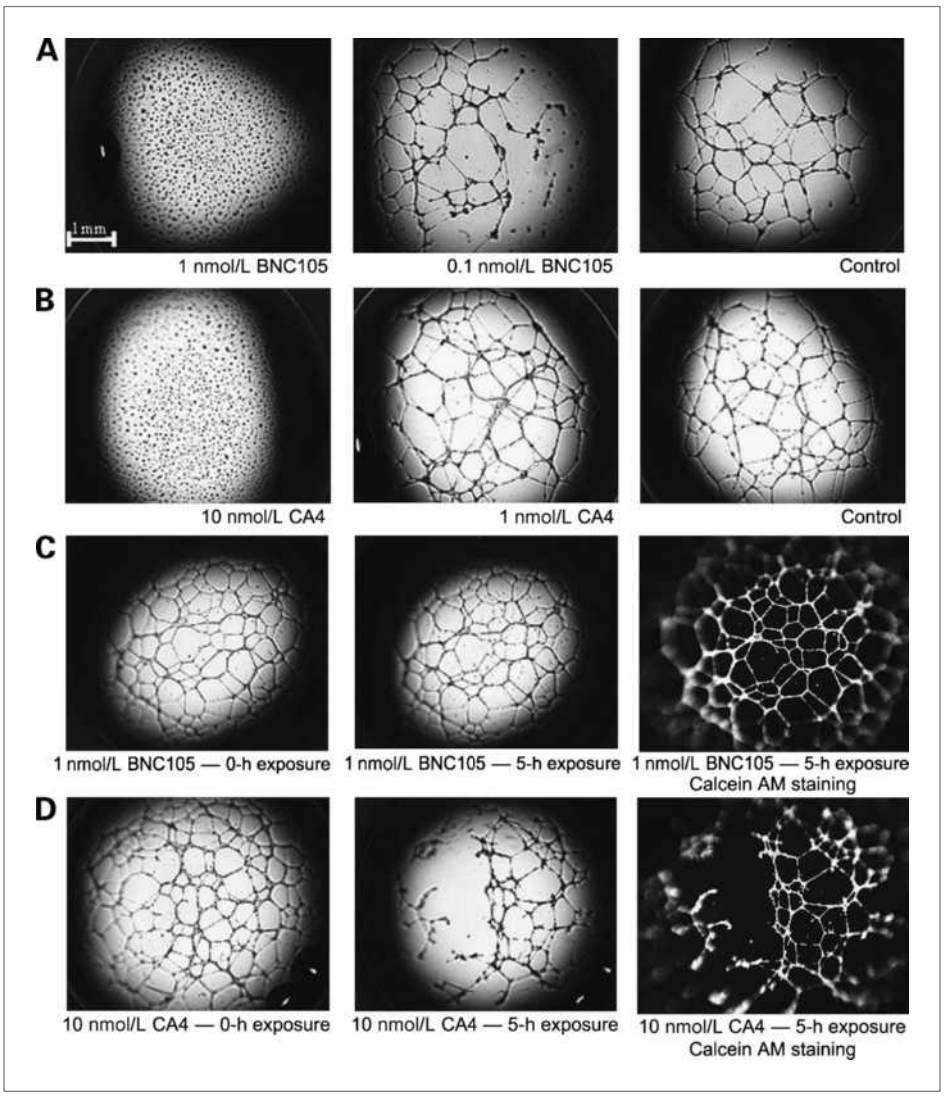

Figure 1. BNC105 selectively inhibits the formation of endothelial cell capillaries but does not affect preformed capillaries. A and B, disruption of capillary formation by BNC105 and CA4. HUVEC and test compound were concurrently added to 96-well plates precoated with Matrigel and incubated for 22 h. C and D, effects of BNC105 and CA4 on stable, preformed capillaries. Preformed capillaries (16 h after HUVEC culture in 96-well Matrigel-coated plates) were treated with varying concentrations of BNC105 and CA4 and monitored for 5 h. Capillaries were stained with calcein AM to verify viable cell structures after 5 h.

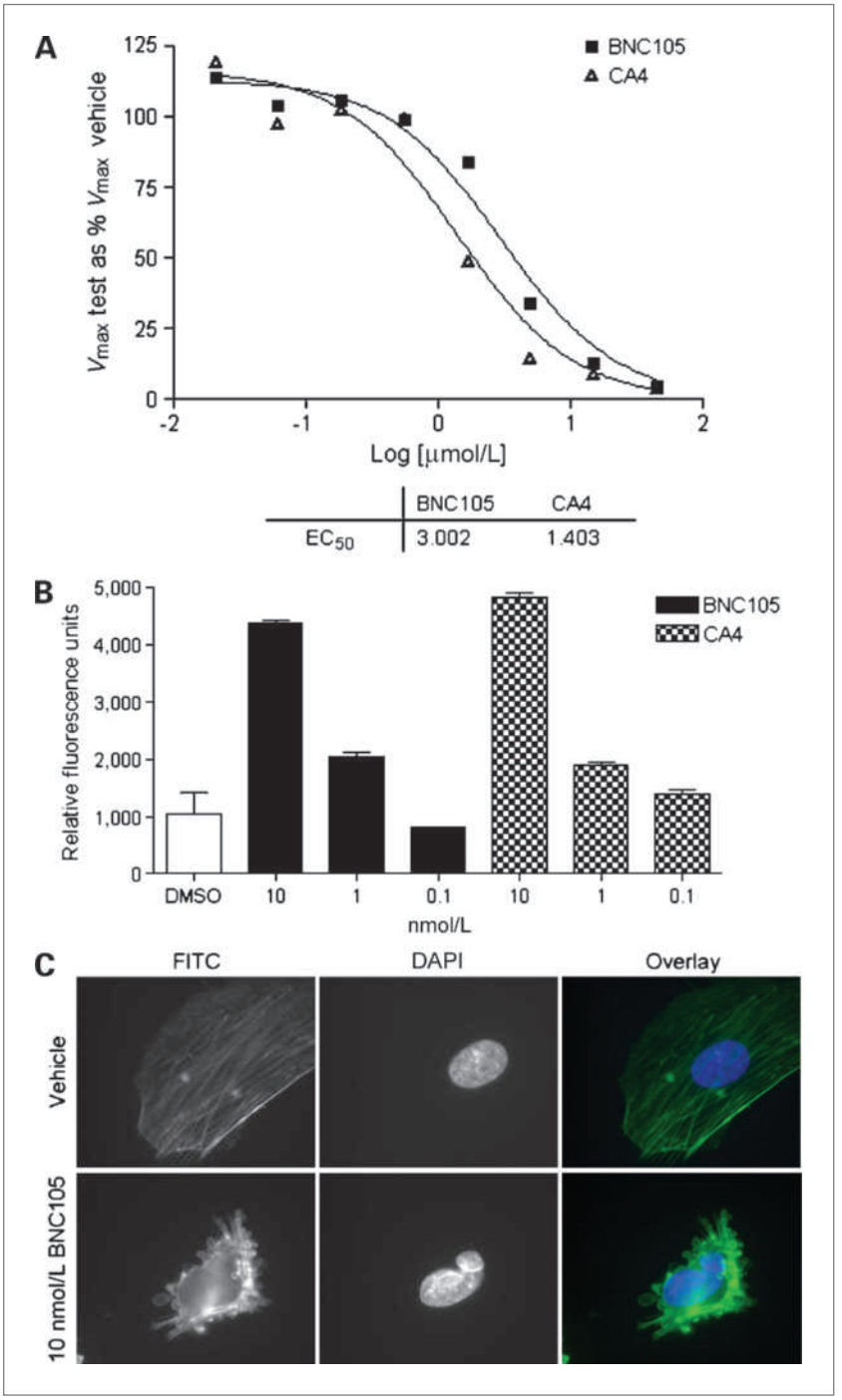

Figure 2. BNC105 exhibits all the hallmarks of a tubulin polymerization inhibitor. A, inhibition of tubulin polymerization by BNC105 (■) and CA4 (▲). Inhibition of the rate of tubulin assembly assessed over a 42-min period was used to determine V_{max} values relative to the control for increasing concentrations of test compound and graphed to determine the EC_{50} for inhibition of bovine tubulin polymerization. B, disruption of endothelial cell monolayer permeability by BNC105 and CA4. Confluent HUVEC monolayers were exposed to BNC105 (black columns) and CA4 (checkered columns) for 15 min. The flow of FITC-conjugated dextran through the monolayer was assessed by relative fluorescence measurements at λ = 485 nm excitation and λ = 530 nm emission in a capture well to determine changes in monolayer permeability following exposure. C, the morphologic changes following 20-min exposure of HUVEC to BNC105 or vehicle (DMSO) were assessed by F-actin staining. FITC-conjugated phalloidin was applied to formaldehyde-fixed cells on glass coverslips and counterstained for nuclei [4′,6-diamidino-2-phenylindole (DAPI)].

BNC105 changes the permeability of endothelial cell monolayers

One of the most important functions of vascular endothelium is to act as a selective barrier to blood solutes. It is anticipated that drugs that interfere with the endothelial cell cytoskeleton may compromise the integrity of endothelial cell layers lining blood vessels. This disruption is likely to result in an increased permeability of the blood vessels. To evaluate the potential effects of BNC105 on vascular permeability, we investigated the consequences of BNC105 exposure on the permeability of confluent HUVEC monolayers grown on microporous membranes. The ability of fluorescent dextran to cross the HUVEC monolayer in the presence of different concentrations of BNC105 or CA4 was assessed. Both BNC105 and CA4 caused an increase in the permeability

of HUVEC monolayers (Fig. 2B). Unlike in the proliferation assay, where the activity of BNC105 is considerably higher than that of CA4 in activated endothelial cell cultures, both compounds seem to be of equal potency in the monolayer permeability assay. This is probably a reflection of the fact that the cells in these confluent monolayers are in a nonproliferating (quiescent) state. This is consistent with the selectivity exhibited by BNC105 for activated/proliferating endothelial cells.

BNC105 induces endothelial cell blebbing

It has previously been shown that CA4 induces cytoskeletal alterations that manifest in a cell blebbing morphology, where actin accumulates around cell membrane micelle-like protrusions (13). To address whether the tubulin polymerization inhibition activity of BNC105 operates via the same mechanism as CA4, HUVEC were exposed to different concentrations (0.1, 1, and 10 nmol/L) of BNC105 and CA4 for 20 minutes. The application of each agent at 10 nmol/L caused cell blebbing (Fig. 2C).

Pharmacokinetics and metabolism of BNC105

To facilitate i.v. administration of BNC105, the phosphate ester of this compound was synthesized (BNC105P; Table 1B) and dissolved in isotonic saline. Plasma pharmacokinetic analysis of BNC105 following i.v. administration of BNC105P was undertaken. Following administration of BNC105P at 6, 18, and 60 mg/kg, BNC105 displayed a C_{max} of 3, 34, and 93 μmol/L and an AUC_{last} of 30, 268, and 814 min·μmol/L, respectively. T_{max} was at 2 minutes, suggesting rapid conversion of BNC105P to BNC105. Metabolism of BNC105 was found to be predominately by the cytochrome P450 CYP2C19 isoform.

BNC105 disrupts the solid tumor vasculature

The efficacy of BNC105 in disrupting tumor vasculature in animals bearing solid tumors derived from human breast (MDA-MB-231), lung (Calu 6), colon (Colo 205), and prostate (DU145) was evaluated. BNC105 was formulated as a disodium phosphate (BNC105P) for i.v. administration. Animals were treated with a single administration of BNC105P. Dose response of tumor vasculature disruption to BNC105P treatment was assessed histologically using H33342 perfusion 24 hours after administration. Complete tumor vascular disruption was observed in all tumor types evaluated at dose levels ≥10 mg/kg (Fig. 3A).

Quantitative analysis of tumor vascular disruption showed that BNC105P achieves statistically significant disruption at dose levels ≥10 mg/kg in all tumor types investigated. The maximum effect was seen in MDA-MB-231 tumors, with efficacy evident at doses as low as 1 mg/kg (Fig. 3B). Staining of tumor sections with H&E enabled quantitative measurement of tumor necrosis resulting from the effects of BNC105. Treatment with BNC105P at 20 mg/kg gave rise to >75% necrosis in MDA-MB-231 tumors. A similar level of necrosis was achieved with CA4P at a considerably higher dose (300 mg/kg; Supplementary Figure 1). Furthermore, in the Colo 205 xenograft model, BNC105P treatment resulted in high degree of tumor vascular disruption with a corresponding level of necrosis that was directly proportional to the dose level of BNC105P. In comparison, CA4P was ineffective in this model (Fig. 3C).

BNC105 alters the solid tumor microenvironment

We undertook a number of histologic analyses to assess the damage caused by BNC105 on the integrity of components within the tumor microenvironment (Fig. 3D). Our analyses included evaluation of the level of apoptosis, the integrity of endothelial cells, and the basement membrane protein laminin. Our observations show that 30 hours after treatment with BNC105, there is a decrease in staining with the CD31 endothelial cell marker, which attests to the destruction of tumor endothelial cells, and a considerable reduction in laminin staining, which is evidence of basement membrane degradation. Furthermore, TUNEL analysis shows a significant increase in the number of apoptotic cells within the tumor. Quantification of TUNEL staining showed that apoptosis in BNC105P-treated tumor sections was approximately eight times higher compared with control (BNC105P, 22.35% of the tumor section area; control, 2.91% of the tumor section area).

BNC105 has a wider therapeutic window than CA4

We investigated the therapeutic window for BNC105 and CA4 as defined by the range between the lowest dose level causing 50% reduction in tumor vascular perfusion and the maximum no observed adverse event level (NOAEL). Acute maximum tolerated dose studies in mice showed a maximum NOAEL of 80 mg/kg BNC105P and 300 mg/kg CA4P. Solid tumors were grown in BALB/c nu/nu mice following injection of the human breast cancer cell line MDA-MB-231 into the mammary fat pad. Mice carrying solid breast tumors were treated with a single i.v. bolus injection of BNC105P at dose levels ranging from 1 to 150 mg/kg or a single dose of CA4P at dose levels ranging from 5 to 400 mg/kg. Twenty-four hours after the injection of the compounds, the animals were injected with the fluorescent dye H33342 before euthanasia. The tumors were excised for histologic examination. Quantitative analyses of H33342 staining in tumor sections revealed that BNC105P treatment caused ~50% vascular shutdown at 1 mg/kg and almost complete vascular shutdown at 10 mg/kg. CA4P required a dose of 100 mg/kg to reach 50% shutdown and a dose of 300 mg/kg to cause 90% vascular shutdown (Fig. 3B).

BNC105 is preferentially retained within solid tumors

The distribution of BNC105 following i.v. administration of 10 mg/kg BNC105P was evaluated in BALB/c nu/nu mice bearing MDA-MB-231 tumors. It was hypothesized that the selective vascular collapse caused by BNC105 in the tumor would result in preferential retention of BNC105 inside the tumor mass. Experimentally,

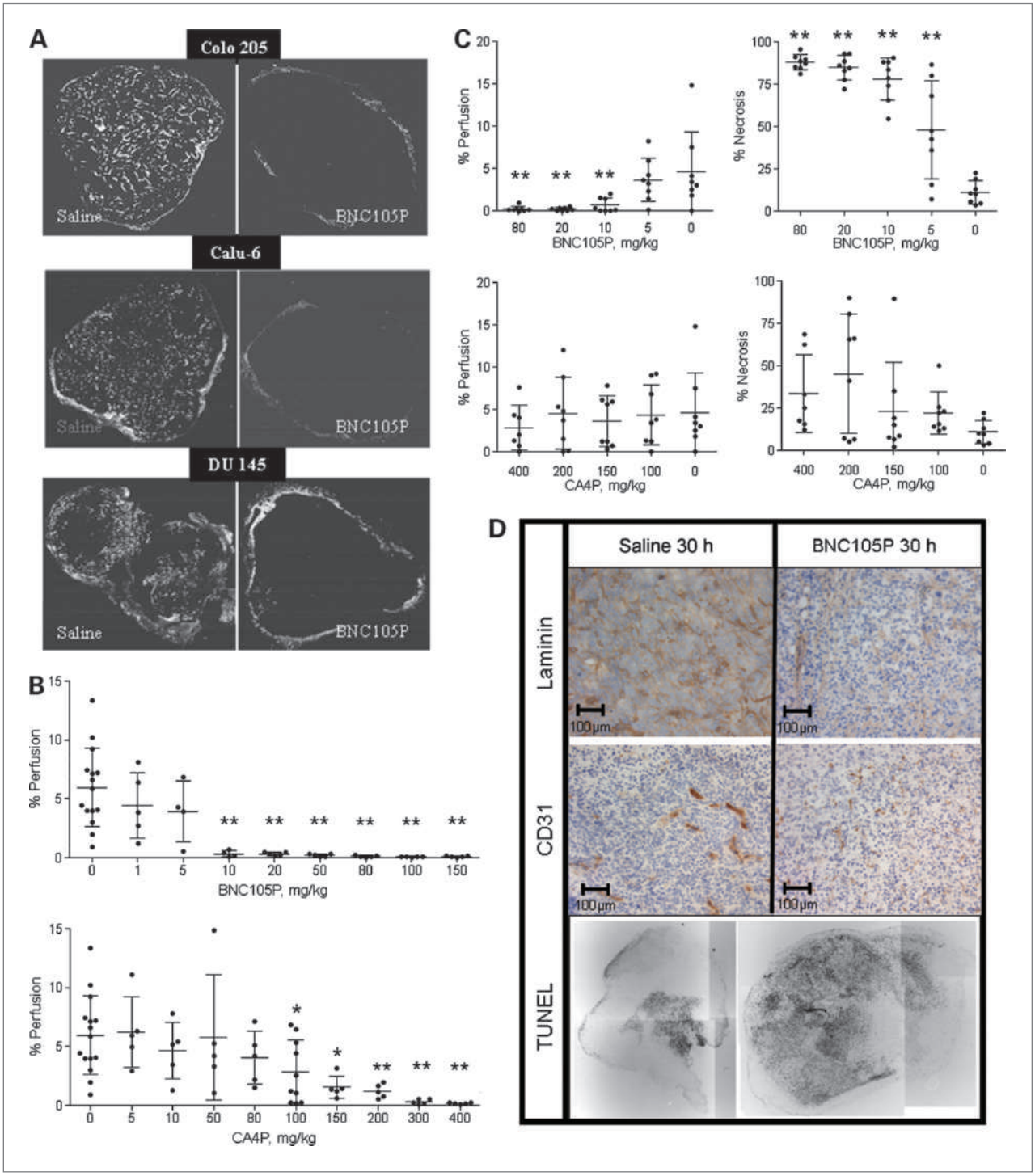

Figure 3. BNC105 is a VDA. A, representative images of H33342 perfusion through Colo 205, Calu 6, and DU145 tumors grown in BALB/c nu/nu mice following treatment with 10 mg/kg BNC105P or saline control. Composite tumor pictures were prepared by tiling multiple images at ×4 magnification to show perfusion throughout the whole tumor section. B, quantitative analysis of vascular shutdown in MDA-MB-231 xenografts. Vascular shutdown was assessed by quantitation of H33342 staining in tumor sections (one section per tumor). A dose-response relationship was established for BNC105P and CA4P. Perfusion was calculated as the percentage of stained area to total tumor area ± SD. *, $P < 0.05$; **, $P < 0.01$. C, assessment of vascular shutdown and necrosis in Colo 205 xenografts with increasing doses of BNC105P. Perfusion throughout the tumor section was quantified by measuring H33342 staining, and necrosis was assessed by H&E staining. Data points represent individual animals ($n = 8$; mean ± SD). **, $P < 0.01$. Perfusion and necrosis were calculated as a percentage of total tumor area. D, representative images of MDA-MB-231 tumors stained for laminin and CD31 (3,3′-diaminobenzidine) counterstained with hematoxylin 30 h after treatment with BNC105P (10 mg/kg) or saline. An *In Situ* Cell Death Kit (TUNEL; Roche) was used to identify cells undergoing apoptosis.

the levels of BNC105 were found to be significantly reduced in all healthy tissues 24 hours after dosing (<5%), yet they remained high in the tumor (64%; Table 2). This is a result of trapping the drug in the tumor following vascular shutdown and may cause a longer exposure time of tumor cells to BNC105.

BNC105 causes solid tumor regression and clearance

We investigated the effect of BNC105P treatment on tumor growth inhibition using a weekly dosing schedule. The logic behind this schedule was to expose the tumor to consecutive cycles of vascular shutdown events. Animals were dosed i.v. with a total of eight doses of BNC105P at 10 mg/kg per dose per week. The data obtained show that BNC105P causes significant suppression of tumor growth (Fig. 4A).

The activity of BNC105P treatment in suppressing tumor growth was compared with that of CA4P in mice bearing MDA-MB-231 tumors. The animals were i.v. treated with BNC105P or CA4P on days 1 and 5 and tumor growth was monitored over a period of 26 days. The suppression of tumor growth achieved with CA4P at 150 mg/kg (one half of the maximum NOAEL) was achieved with BNC105P at 10 mg/kg (one eighth of the maximum NOAEL; Supplementary Figure 2).

Based on the wide therapeutic window captured by BNC105, we evaluated the tumor growth inhibitory activity of BNC105 at dose levels higher than 10 mg/kg. It was hypothesized that at higher dose levels, BNC105 may achieve tumor regression by enlisting both the antivascular and the antimitotic activities inherent to its mechanism of action. Repeat administrations at doses ranging from 10 to 80 mg/kg showed that BNC105P is not tolerated at dose levels $\geq$60 mg/kg. At dose levels $\leq$40 mg/kg, BNC105P was well tolerated. Animals bearing Calu 6 (lung cancer) human tumors were treated with two administrations of BNC105P 1 week apart at 40 mg/kg. BNC105 displayed significant tumor growth inhibition in this tumor model (Fig. 4B).

Mice bearing MDA-MB-231 solid tumors were treated with two weekly doses of BNC105P at the start of each of two 37-day cycles of dosing. The dose level of 40 mg/kg produced an average 52% regression in tumor size in the first 2 weeks posttreatment and a prolongation in suppression of tumor growth up to day 95 (mean of 544.19 mm^3, SD ± 921.37 mm^3) versus saline control (mean of 1745.68 mm^3, SD ± 1,444.97 mm^3 at day 51 when these animals were euthanized). A subsequent study investigated the effect of a 28-day dosing cycle with BNC105P administration at 40 mg/kg on day 1 and day 8 of each cycle. Mice bearing MDA-MB-231 solid tumors were dosed for a total of three cycles. This treatment regimen resulted in significant tumor growth suppression, with a number of treated animals experiencing tumor regression or being cleared of their tumor burden (Fig. 4C).

To confirm and further substantiate these findings, we evaluated this dosing regimen using a larger number of animals bearing tumors that varied in size between 200 and 600 mm^3. Animals were treated with two 28-day cycles of BNC105P at 40 mg/kg. Significant differences in tumor growth between BNC105P-treated (n = 64) and saline-treated (n = 20) animals were observed as early as day 4 ($P < 0.001$, unpaired t test; Prism analysis) through to day 70. In the BNC105P-treated group, 34% of tumors showed significantly delayed growth, 4.7% exhibited no growth, 6.3% regressed, and 14% of tumors were cleared. Figure 4D depicts a BALB/c nu/nu mouse in which tumor growth was arrested and the tumor disappeared by day 60 of BNC105P two-cycle treatment. Cleared tumors did not reappear for the duration of the study.

Discussion

The dependency of solid tumors on blood supply for growth and metastasis has provided the impetus for

Table 2. BNC105 is selectively retained within tumors following administration of BNC105P

Organ	BNC105 concentration (ng/mL) after i.v. administration of BNC105P				% BNC105 remaining 24 h after administration of BNC105P [BNC105 (24 h) / BNC105 (0.25 h) × 100]
	0.25 h	2 h	6 h	24 h	
Tumor	416	327	349	267	64
Liver	345	135	84	<LLQ	0
Heart	474	234	77	24	5
Spleen	1866	835	355	28	2
Kidney	733	361	159	30	4
Brain	1762	1263	782	77	4

NOTE: Organs and tumors from animals treated with 10 mg/kg BNC105P were removed and the BNC105P derivative compound BNC105 was extracted. The concentration of BNC105 was determined using HPLC-MS and is reported as nanograms per milliliter. The percentages of BNC105 remaining in the tumor and normal organs after 24 h were calculated.
Abbreviation: LLQ, Lower Limit of Quantification.

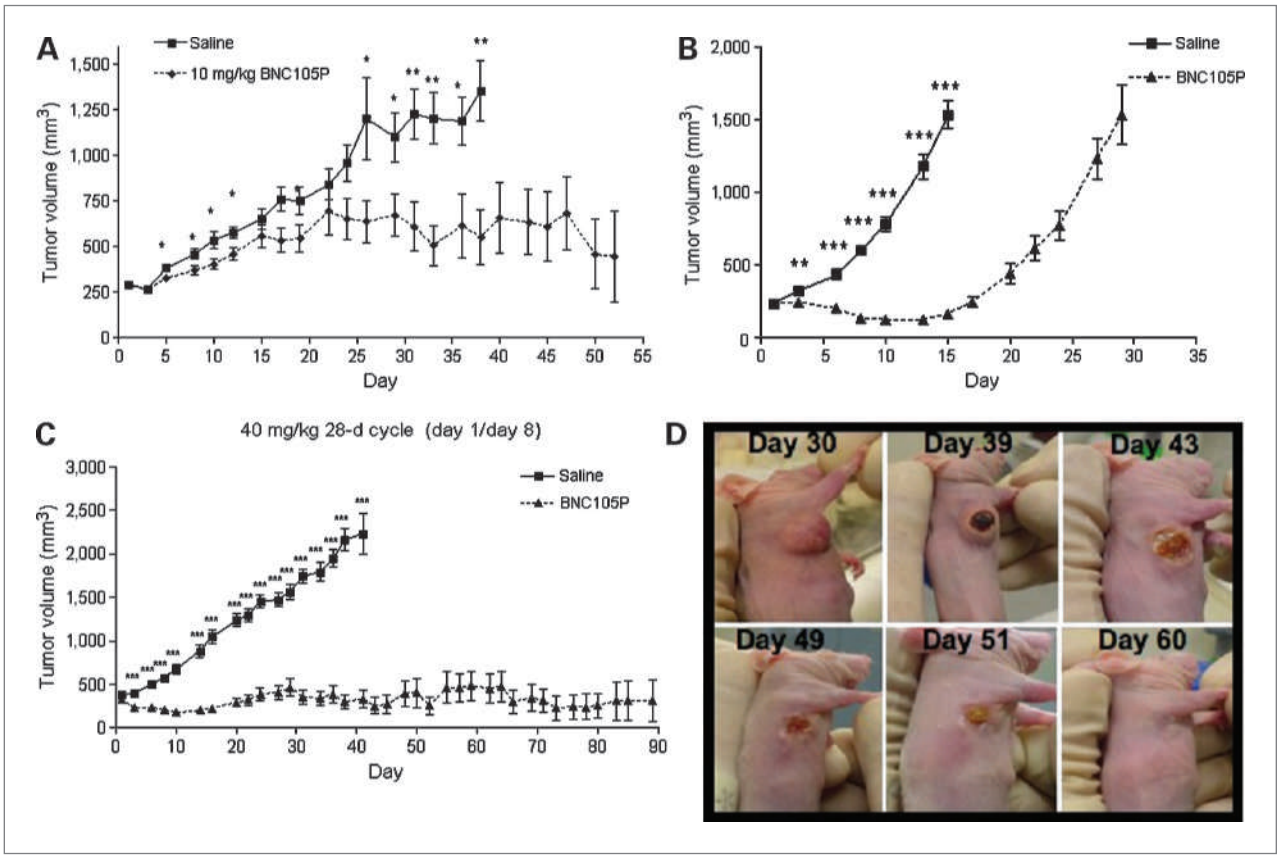

Figure 4. BNC105 causes significant tumor growth inhibition. A, *in vivo* tumor growth inhibition activity of BNC105 in the MDA-MB-231 breast carcinoma model. Animals (n = 10) were treated weekly with 10 mg/kg BNC105P (▲) or saline vehicle control (■; mean ± SEM). Treatment was administered on days 1, 8, 15, 22, 29, 36, 43, and 50. Significant differences in tumor volume of treated group as determined by two-tailed t test are indicated (*, $P < 0.05$; **, $P < 0.01$; ***, $P < 0.001$). B, *in vivo* tumor growth inhibition activity of BNC105 in the Calu 6 (lung anaplastic carcinoma) xenograft model. Animals (n = 10) were treated with 40 mg/kg BNC105P (▲) or saline vehicle control (■) on days 1 and 8 and tumor volume was measured (mean ± SEM). Significant differences in tumor volume of treated group as determined by two-tailed t test are indicated by (*, $P < 0.05$; **, $P < 0.01$; ***, $P < 0.001$). C, tumor growth suppression in MDA-MB-231 breast tumors following treatment with BNC105P. Animals (n = 10) were treated with 40 mg/kg BNC105P (▲) or saline vehicle control (■) on days 1, 8, 29, 36, 64, and 71 (mean ± SEM). Significant differences in tumor volume of treated group as determined by two-tailed t test are indicated (*, $P < 0.05$; **, $P < 0.01$; ***, $P < 0.001$). D, representative images obtained from a MDA-MB-231 tumor–bearing mouse that experienced tumor clearance following four doses of BNC105P treatment at 40 mg/kg.

targeting the vasculature that supports tumor growth. Vascular targeting strategies include the suppression of new blood vessel formation using inhibitors of angiogenesis and the disruption of established blood vessels using VDAs. Antiangiogenic agents require chronic administration and operate through prevention of neovascularization. VDAs are more suited to acute administration and achieve immediate vascular damage effects. VDAs exert their effects by increasing permeability and interstitial fluid pressure, leading to plasma leakage, blood vessel diameter reduction, decreased blood flow, and vascular shutdown. There are currently a number of tubulin polymerization inhibitors in clinical development as VDAs. CA4P has progressed through to phase III clinical trials, and AVE8062 (Sanofi-Aventis) has been reported to be in phase III evaluation for advanced-stage soft tissue sarcoma after failure of anthracycline and ifosfamide chemotherapies (trial NCT00699517). Other compounds include OXi4503 (14), NPI-2358 (15), CYT-997 (16), MPC-6827 (17), and EPC2407 (18, 19). These latter agents have completed phase I evaluation and are under evaluation in phase II trials. The number of compounds being evaluated in this arena attests to the potential utility of the VDA approach. Many efforts are aimed at identifying agents that improve on the therapeutic capacity of CA4P by attaining a wider therapeutic window. The most frequently reported DLT events reported for this class of compounds (acute coronary and/or thrombophlebotic events, blood pressure, and heart rate changes) are consistent with their mechanism of action. In an attempt to identify compounds that offer a wider therapeutic window, we used *in vitro* screening assays that exploit the differentiating features in activated endothelial cells compared with endothelial cells that are in a quiescent state.

The discovery of BNC105 was based on its selectivity for endothelial cells that are in a state of active proliferation or

angiogenesis. BNC105 is far less potent against cells in a quiescent state, as shown in two independent *in vitro* assay paradigms. Endothelial cells actively proliferating in culture were found to be highly susceptible to the action of BNC105, whereas nonproliferating endothelial cells were 80 times less sensitive. Interestingly, CA4 did not exhibit selectivity for the actively proliferating endothelial cell cultures. This is in contrast to previous reports showing that CA4 exhibits selectivity for proliferating over confluent nonproliferating endothelial cells. This is likely to reflect differences in culture conditions used in the assay. The cell culture described here compares exponentially growing endothelial cell cultures maintained in standard medium with all necessary growth factors to viable nonproliferating growth factor–deprived endothelial cell cultures. In comparison, prior reports of CA4 selectivity were based on culture systems where nonproliferating cultures were obtained through contact inhibition and the use of media derived from cancer cell cultures under hypoxic conditions (20).

To further substantiate the selectivity seen with BNC105, we used a different *in vitro* assay that is dependent on cytoskeletal differences in endothelial cells engaged in forming capillary tubes compared with those in preformed stable capillaries. Consistent with the selectivity displayed for actively proliferating endothelial cells, BNC105 displayed selective action against cells engaged in capillary tube formation. This selectivity was not observed with CA4.

The activity of BNC105 in a number of *in vitro* assays showed the hallmarks of a tubulin-targeting compound (13, 21). BNC105 inhibits *in vitro* tubulin polymerization, induces increases in permeability in endothelial cell monolayers, and causes endothelial cell blebbing. The effects of BNC105 on cell blebbing and endothelial cell monolayer permeability suggest that the ability of BNC105 to act as a VDA is through its effects on the endothelial cell cytoskeleton. In subcutaneous solid tumor animal models, BNC105 behaved as a classic tubulin polymerization inhibitor causing reduction in tumor vascular perfusion, leading to destruction of tumor vessels. This was evidenced by a decrease in laminin and CD31 staining as well as considerable tumor cell necrosis.

Consistent with its *in vitro* efficacy against activated endothelial cells, BNC105 was a potent VDA within solid tumors of human cancer origin. To facilitate i.v. administration, BNC105 was formulated as a disodium phosphate prodrug (BNC105P), an approach previously reported for CA4 (CA4P; ref. 20). Plasma pharmacokinetic analysis of BNC105 following i.v. administration of BNC105P showed that BNC105P is rapidly converted to BNC105. Partial VDA activity was seen at dose levels as low as 1 mg/kg BNC105P, with complete vascular disruption seen in all cell lines evaluated at dose levels ≥10 mg/kg. Compared with CA4P, BNC105P is more effective and offers a wider therapeutic window as defined by the minimum single administration dose level that causes >95% vascular shutdown and the maximum NOAEL dose. CA4P produced 90% vascular disruption at its NOAEL, whereas BNC105P produced 95% vascular disruption at a dose level eight times lower than its NOAEL.

Evaluation of the effects of BNC105 on tumor growth inhibition have shown that this agent has significant efficacy in a breast cancer model when administered at a 10 mg/kg (minimum dose level causing >95% vascular disruption) repeat dose schedule. Furthermore, significantly enhanced tumor growth inhibition was seen when dosing was increased to 40 mg/kg per dose. Two 40 mg/kg doses of BNC105P administered 1 week apart yielded significant tumor growth inhibition in a model of human lung (Calu 6) cancer. Furthermore, tumor regressions and tumor burden clearance were observed in animals bearing MDA-MB-231 human breast cancer tumors following treatment with four 40 mg/kg BNC105P doses over two 28-day cycles. This result is consistent with a dramatic ischemic/necrotic effect on the tumors that surmounts any counter-response from the tumor cells. Based on its large therapeutic window, it is reasonable to believe that BNC105 can be administered at dose levels that combine a VDA effect with direct cytotoxic activity due to inhibition of tubulin dynamics. Analysis of BNC105 tissue distribution following administration of BNC105P showed that BNC105 is preferentially retained within the solid tumor mass compared with other normal tissues. The longer retention of BNC105 in the tumor mass relative to normal organs shows trapping of the compound inside the tumor as a consequence of vascular shutdown, and provides for longer exposure of cancer cells to BNC105, yielding significant single-agent efficacy.

It is reasonable to suggest that the strong tumor-suppressive activity exhibited by BNC105 is a product of several antitumor effects exerted on growing solid tumors. The data presented in this report show that BNC105 exhibits antiproliferative activity and also seems to be a strong inhibitor of capillary formation by endothelial cells in culture, suggesting antiangiogenic activity. Furthermore, through induction of cytoskeletal changes, BNC105 acts as a potent disruptor of tumor vasculature. All these effects are potentially further enhanced through prolonged tumor-site drug exposure arising from the demonstrated preferential retention of BNC105 within solid tumors.

In summary, by using two independent *in vitro* assays that differentiate between activated and quiescent endothelial cells, we identified BNC105, a novel tubulin-targeting agent that exhibits selectivity for activated endothelium. BNC105 causes strong tumor vascular disruption and exhibits single-agent efficacy in a number of xenograft tumor models. BNC105 is currently under evaluation in a phase I clinical trial.

Disclosure of Potential Conflicts of Interest

All authors are employees of Bionomics Ltd.

The costs of publication of this article were defrayed in part by the payment of page charges. This article must therefore be hereby marked *advertisement* in accordance with 18 U.S.C. Section 1734 solely to indicate this fact.

Received 09/01/2009; revised 02/23/2010; accepted 03/23/2010; published OnlineFirst 06/01/2010.

References

1. Pellegrini F, Budman DR. Review: tubulin function, action of antitubulin drugs, and new drug development. Cancer Invest 2005;23: 264–73.
2. Han Y, Malak H, Chaudhary AG, Chordia MD, Kingston DG, Bane S. Distances between the paclitaxel, colchicine, and exchangeable GTP binding sites on tubulin. Biochemistry 1998;37:6636–44.
3. Pasquier E, André N, Braguer D. Targeting microtubules to inhibit angiogenesis and disrupt tumour vasculature: implications for cancer treatment. Curr Cancer Drug Targets 2007;7:566–81.
4. Hait WN, Rubin E, Goodin S. Tubulin-targeting agents. Cancer Chemother Biol Response Modif 2005;22:35–59.
5. Tozer GM, Kanthou C, Baguley BC. Disrupting tumor blood vessels: tubulin-binding agents and the combretastatins. Nat Rev Cancer 2005;5:423–35.
6. Salmon B, Siemann D. Characterizing the tumor response to treatment with combretastatin A4 phosphate. Int J Radiat Oncol Biol Phys 2007;68:211–17.
7. Kanthou C, Tozer MT. Microtubule depolymerizing vascular disrupting agents: novel therapeutic agents for oncology and other pathologies. Int J Path 2009;90:284–94.
8. Dowlati A, Robertson K, Cooney M, et al. A phase I pharmacokinetic and translational study of the novel vascular targeting agent combretastatin A-4 phosphate on a single-dose intravenous schedule in patients with advanced cancer. Cancer Res 2002;62:3408–16.
9. Lo Russo PM, Gadgeel SM, Wozniak A, et al. Phase I clinical evaluation of ZD6126, a novel vascular-targeting agent, in patients with solid tumors. Invest New Drugs 2008;26:159–67.
10. Bussolati B, Deambrosis I, Russo S, Deregibus MC, Camussi G. Altered angiogenesis and survival in human tumor-derived endothelial cells. FASEB J 2003;17:1159–61.
11. Watts ME, Woodcock M, Arnold S, Chaplin DJ. Effects of novel and conventional anti-cancer agents on human endothelial permeability: influence of tumor secreted factors. Anticancer Res 1997;17:71–75.
12. Trotter MJ, Olive PL, Chaplin DJ. Effect of vascular marker hoechst 33342 on tumor perfusion and cardiovascular function in the mouse. Br J Cancer 1990;62:903–8.
13. Kanthou C, Tozer GM. The tumor vascular targeting agent combretastatin A-4-phosphate induces reorganization of the actin cytoskeleton and early membrane blebbing in human endothelial cells. Blood 2002;99:2060–9.
14. Hua J, Sheng Y, Pinney KG, et al. Oxi4503, a novel vascular targeting agent: effects on blood flow and antitumor activity in comparison to combretastatin A-4 phosphate. Anticancer Res 2003;23: 1433–40.
15. Nicholson B, Lloyd GK, Miller BR, et al. NPI-2358 is a tubulin-depolymerizing agent: *in vitro* evidence for activity as a tumor vascular-disrupting agent. Anticancer Drugs 2006;17:25–31.
16. Burns CJ, Harte MF, Bu X, et al. Discovery of CYT997: a structurally novel orally active microtubule targeting agent. Bioorg Med Chem Lett 2009;19:4639–42.
17. Kasibhatla S, Baichwal V, Cai SX, et al. MPC-6827: a small-molecule inhibitor of microtubule formation that is not a substrate for multidrug resistance pumps. Cancer Res 2007;67:5865–71.
18. Cai SX. Small molecule vascular disrupting agents: potential new drugs for cancer treatment. Recent Pat Anticancer Drug Discov 2007;2:79–101.
19. Cai SX, Drewe J, Kemnitzer W. Discovery of 4-aryl-4*H*-chromenes as potent apoptosis inducers using a cell- and caspase-based anti-cancer screening apoptosis program (ASAP): SAR studies and the identification of novel vascular disrupting agents. Anticancer Agents Med Chem 2009;9:437–56.
20. Dark GG, Hill SA, Prise VE, Tozer GM, Pettit GR, Chaplin DJ. Combretastatin A-4, an agent that displays potent and selective toxicity towards tumor vasculature. Cancer Res 1997;57: 1829–34.
21. El-Emir E, El-Emir E, Boxer GM, et al. Tumour parameters affected by combretastatin A-4 phosphate therapy in a human colorectal xenograft model in nude mice. Eur J Cancer 2005;41:799–806.